PAPER

Open-source 3D printed laboratory for education: illuminating optics and optoelectronics demonstrations

To cite this article: Raj K Vinnakota *et al* 2024 *Phys. Educ.* **59** 025005

PAPER

Phys. Educ. **59** (2024) 025005 (17pp) iopscience.org/ped

Open-source 3D printed laboratory for education: illuminating optics and optoelectronics demonstrations

Raj K Vinnakota[1,*], **Brady A Barr**[1] **and Sai Radavaram**[2]

[1] Department of Chemistry and Physics, TROY University, Troy, AL 36082, United States of America
[2] Engineering Department, Utah Tech University, St. George, UT 84779, United States of America

E-mail: rvinnakota@troy.edu and rajk.vinnakota@gmail.com

Abstract
This article introduces a flexible and reliable tabletop setup, specifically designed to effectively demonstrate fundamental optics concepts to a wide audience, including students from grades 5 through 12, university students, as well as enthusiasts. Leveraging additive manufacturing technology, this work provides an adaptable and accessible avenue for educators, students, and enthusiasts to explore the captivating realm of optics and optoelectronics. The article delves into detailed discussions of the experiments that can be conducted with the proposed setup to elucidate these concepts, presenting their outcomes comprehensively. Moreover, all the Computer Aided Design (CAD) files utilized in this project for 3D printing the essential optical components and systems are made available online for free, enabling users to develop the setup from scratch independently. The proposed setup offers an easily approachable design process, requiring minimal to no prior CAD experience. The experiments performed to illustrate optical concepts are straightforward and safe, making them easily comprehensible and achievable for students at various educational levels.

Keywords: additive manufacturing, 3D optical bench setup, optics and optoelectronics experiments

* Author to whom any correspondence should be addressed.

1. Introduction

The field of optics is expansive and captivating, spanning across disciplines such as Physics, Engineering, Material Sciences, and Chemistry. Its concepts find practical applications in our daily lives, touching areas like optical fibres, surgical tools, contact lenses, microscopes, lasers, and optoelectronics [1–4]. The global optoelectronics market, estimated at USD 6.54 billion in 2022, is projected to exceed USD 21.2 billion by 2032 [5], indicating a promising market trend. Despite this, there's still a need for skilled technicians in optics and photonics, partly because fewer students are enrolling in related postsecondary programs [6]. This enrolment decline can be associated, at least in part, with the intricate nature of traditional optics coursework. Many students find it challenging to grasp due to the imaginative demands and the necessity for 2D/3D visualization of light generation, propagation, and interaction in various mediums [7, 8]. Overcoming these challenges involves recognizing that optics and photonics education can benefit from specialized lab equipment, like tables, laser sources, and spectrum analysers, which may not be readily available in K-12 schools or non-specialized engineering institutions [9]. While alternative teaching methods [10–16], educational kits [16–25], and virtual tools [26–29] help to some extent by facilitating hands-on and visual demonstrations, they have some limitations. These include a lack of customization, limited design flexibility, and the inability to integrate additional components for advanced experiments. To address these limitations, we explore an adaptable laboratory and pedagogical tool with the possibility to engage students at different complexity levels in optics and photonics education, while also facilitating in-class concept demonstrations. Additionally, the authors posit that this approach might also benefit homeschooling students, offering access to otherwise challenging resources and learning experiences. Notably, this aligns with the increasing global trend in homeschooling [30], which has seen exponential growth post-COVID-19 pandemic, particularly in the United States, with nearly a 3% annual increase [31].

In the past decade, significant strides in additive manufacturing, often referred to as 3D printing, have brought forth the remarkable ability to design, create, and test customized parts within the confines of a tabletop environment. This technology has not only permeated various industries like Aerospace [32], Automotive [33], Architecture [34], and Biomedical [35] for rapid prototyping but is also gradually making its way into the educational sector. In the field of chemistry education, for instance, 3D printed models play a pivotal role in showcasing macroscopic representations of atomic [36, 37], molecular [38, 39], and crystallographic unit cell structures [40], as well as potential surfaces [41] and proteins [42]. Similarly, within the domain of mechanical engineering education, 3D printing finds applications across diverse spheres such as design, prototyping [43], manufacturing [44], validating simulated models [45], and robotics [46]. In electrical engineering education, the application of 3D printed models holds immense value by providing visual representations of intricate electrical pathways that would otherwise present considerable challenges [47]. Moreover, the concept extends to fabrication of on-demand components for use in supportive laboratory environments [48]. Furthermore, the capabilities of 3D printing expand into research laboratories, where it plays a role in configuring experimental setups for diverse objectives such as THz range spectroscopic analyses [49, 50] and imaging fluorescence microscopes [51].

Within the context of optics, Zhang *et al* [52] have showcased a series of designs encompassing optical holders for lenses, filters, mirrors, fibre optics, and optical positioners tailored to an optical rail system. Their work encompassed 3D printing these optical mounts for both research and educational purposes. Similarly, Davis *et al* [53] proposed models designed specifically for an upper-division instrumental analysis laboratory course. They presented a range of 3D printed optical mounts, posts, holders, and hardware intended to complement a traditional optical breadboard setup. While the efforts in [52] and [53] are commendable, their designs exhibit a lack of generality. These designs are optimized for specific applications—Zhang *et al*'s designs for an optical rail system suited for physics education and Eric *et al*'s designs for chemical education and instrumentation—both still relying on costly optical breadboards and rail systems. In our endeavour, we strive to contribute to the existing database and bridge a resource gap for those using 3D printers within optics and photonics education.

In this manuscript, we introduce a customizable Optical LEGO bench setup that comprises a set of modular optical breadboards with screw-in pegs, mounts, posts, holders, and additional hardware. Our focus in this work is on providing components that cater to basic and intermediate optics and photonics experiments. Through the implementation of these 3D printed optical components, we conducted a diverse range of experiments. These experiments covered fundamental optical concepts such as reflection, refraction, light behaviours through convex and concave lenses, observation of the optical interference using red, blue, and green wavelengths resulting in a rainbow-like spectrum, light diffraction properties, energy conversion with solar cells, total internal reflection, optical fibre light guidance phenomena, light emitting diodes (LEDs) I–V characteristics, and photodetection using photodiodes and phototransistors. Notably, our approach offers flexibility for expansion as needed. Educators, instructors, or students with minimal Computer Aided Design (CAD) and 3D printing experience can easily create and fabricate new components to suit specific course requirements, concept demonstration, or laboratory needs. This methodology finds applicability in various contexts, including lower division laboratory courses aimed at instructing optics to general science students. Furthermore, it can be seamlessly adapted to upper division optics and optoelectronics labs. However, expanding to these levels demands a solid proficiency in CAD and prototyping to design functional prototypes. We firmly believe that this portable 3D printed optical bench setup offers significant advantages. It can adeptly (i) showcase and explain optics and photonics concepts to primary and secondary students, potentially igniting their enthusiasm for STEM subjects, and (ii) facilitate the assimilation of fundamental optics into everyday life, nurturing inquiry-based thinking among students.

2. Design and 3D printing of optical components

The 3D CAD models of all components and mounts used in the optical bench setup were designed utilizing Autodesk Fusion 360 [54]. The choice of Fusion 360 was guided by its user-friendly interface and parametric modelling capabilities, which are particularly beneficial for industrial and engineering design. Additional factors for choosing Fusion 360 include the availability of free one-year educational access for students and educators, which is renewable as long as they remain eligible [55]. In the spirit of fostering open-source collaboration, all generated CAD models (.F3D files) as well as 3D model file formats (.STL and .STEP) have been made readily available online [56]. For the physical realization of these components, the Creality CR-10 V3 printer [57] was employed, with Ultimaker Cura [58] serving as the slicing software to generate standard *.GCODE files for the printer. The chosen printing material, or filament, was a 1.75 mm diameter polylactic acid plastic, a popular choice in 3D printing due to its favourable mechanical and thermal attributes. The printing parameters remained consistent across all iterations, with a nozzle temperature of 200 °C and a print bed temperature of 60 °C. For the majority of the prints, an infill density of 15% was used, while specific models like screws necessitated a density of 100% to enhance durability. These settings resulted in varying print times, typically ranging from 0.5 to 2 h. However, breadboards took approximately 4 h to print. It is important to note that while these specified settings and materials consistently yielded successful parts, variations in filament or printer choice may require adjustment to the parameters.

Figure 1 showcases the list of the essential components that were designed, and 3D printed for conducting the experiments discussed in the following section. Figure 1(a) highlights the modular optical breadboard, measuring 1 in.×1 in., and featuring external slots. This breadboard functions as a foundational platform to mount

Figure 1. 3D design and printed components: (a) modular optical breadboard featuring screw-in holes compatible with ¼ inch screws. The insert highlights the arrangement of screw holes. (b) Breadboard pegs. (c) Optical mounts. (d) Mounts specifically designed to accommodate LED circuitry and an 9 V battery. (e) Mount crafted to encase the solar cell circuitry along with an LED indicator. (f) Mount tailored to accommodate a flashlight or laser source of 38 mm diameter. (g) Mount engineered to hold a 75 mm × 75 mm reflective mirror. (h) Mount designed to house a 51.50 mm × 51.25 mm diffraction grating. (i) Rectangular prism mount with a cross-sectional width of 26.15 mm. (j) Mount crafted to encase the rectangular prism (k) components include a height-adjustable laser mount, circular and rectangular PCB holders, and a laser holder with adjustable diameter for precise laser source positioning and PCB handling.

additional experiment components. Notably, the 3D printer's limitations led us to create smaller segments of the breadboard, allowing for expansion by locking in extra sections, much like LEGO blocks. This approach offers several advantages: firstly, in the event of precision or fabrication errors, only the affected segment needs reprinting, saving time and material costs. Secondly, it provides flexibility in expanding the board size horizontally or vertically, which would be unfeasible with a single large optical breadboard. It is worth noting that while our design shares some visual resemblance with previous work [53], our version incorporates screw-in assemblies to secure other optical components. Figure 1(b) presents the Breadboard pegs, pivotal for holding the optical mounts and posts. These pegs boast a screw thread of an inch in length and a shank spanning an inch. Furthermore, the design incorporates (as shown in the insert of figure 1(b)) a top slot that permits the use of a screwdriver for insertion into the breadboard. We opted for this design for two key reasons: firstly, to firmly secure optical mounts and holders, and secondly, to enable unimpeded rotation of these components. Figure 1(c) showcases the optical mounts for accommodating 38 mm diameter lenses. Their design includes a flush case for effortless lens placement and exchange. Diverse post holders are depicted in figures 1(d)–(J), each tailored to specific functions, which will be explained in detail in the following section. Figure 1(k) provides a visual representation of the height-adjustable mount, featuring mounts for circular (20 mm) PCB modules on which light-dependent resistor (LDR), LED, photodiode, and phototransistor are soldered. These components are designed for optoelectronic experiments, enabling observations of laser diode and LED characteristics, as well as those of photodiodes, phototransistors, and photoresistors. Furthermore, an additional mount is incorporated to firmly secure the laser diameter within the laser mount. This supplementary mount is to adjust the laser source diameter to precisely align with the dimensions of the laser diode mount. All optical mounts and post holders feature a small 10.5 mm hole at their base (see insert in figure 1(F) to facilitate easy snap-on connection with the shank side of the mounting pegs. This arrangement grants a full 360° range of motion.

3. Results and discussion

3.1. RGB colour mixing and rainbow-like spectrum

The red, green, blue (RGB) colour mixing experiment delves into the fundamental principle of additive light colour mixing. It demonstrates the synthesis of white light through the combination of distinct red, blue, and green wavelengths of light. Furthermore, this experiment facilitates the exploration of secondary colours such as cyan, magenta, and yellow. To visually illustrate the colour mixing phenomenon using red, blue, and green light, the experiment incorporates custom-designed LED light posts, as shown in figure 1(d). These 3D-printed LED light posts house essential circuitry (see insert in figure 2(C)), including a 100 Ω series resistor, an ON/OFF switch, a 9 V battery, and connecting wires. The casing accommodates a small convex plastic lens and an LED holder to securely position the LED, while also allowing for convenient component replacement.

As shown in figure 2(A), the experimental setup involves positioning the RGB LED light posts at a designated distance from a white screen. The process includes inserting the convex lens into the specified mount, as depicted in figure 1(C). This convex lens post is then placed between the white screen and the LED posts. By carefully adjusting (slightly rotating) the positions of the LED light posts, the emitted light is directed through the convex lens. With careful and precise adjustments (by slightly rotating), the positions of the LED light posts are manipulated. This slight adjustment ensures that the emitted light is directed through the convex lens. As the converged light rays follow their path, they are projected onto the screen, creating an overlapped additive display, as depicted in the inset of figure 2(B). Nevertheless, the image suggests that the blue light is overpowering the green and red lights, although this discrepancy is not evident when directly observing with the naked eye. The discrepancy may be because we used a regular camera, not a professional one. It is important to note that this photo was taken with an iPhone 13. Additionally, the fixed series resistance in the LED circuit ensures a steady light intensity, while introducing a potentiometer provides the opportunity for precise control over current flow and, consequently, light intensity.

A rainbow-like spectrum can result from the interference of RGB light, known as 'iridescence' or 'interference colours.' This phenomenon arises as light waves interact with each other and with material surfaces, leading to constructive and destructive interference. To illustrate this, we utilize a rectangular transparent prism mounted on a prism mount (refer to figure 1(j)). When crafting the design for the prism mount, its length is carefully adjusted to align with the dimensions of both the prism and the LED light posts. This approach ensures a seamless fit and accurate alignment within the experimental setup. To visualize the rainbow-like spectrum, the experimental

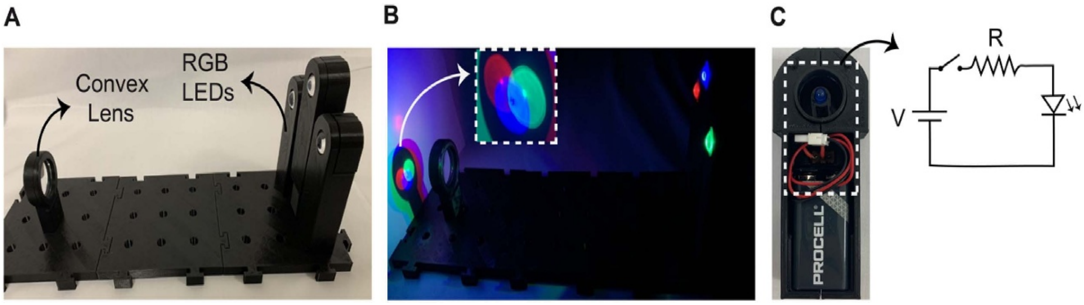

Figure 2. (A) Experimental arrangement demonstrating RGB colour mixing. (B) Outcome illustrating the achieved near colour mixing phenomenon; the inset illustrates the observed mixing effect. (C) Electrical circuit of lighting up LED, $V = 9$ V, $R = 100\ \Omega$.

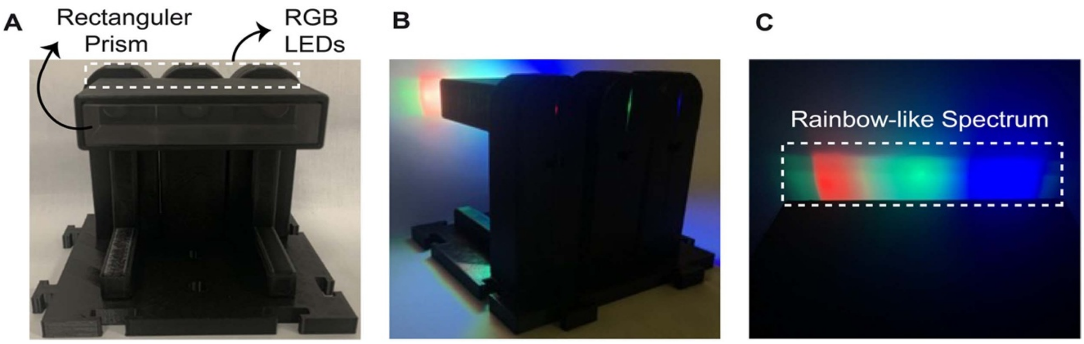

Figure 3. (A) Experimental configuration showcasing RGB interference and the observation of a rainbow-like spectrum. (B) and (C) Results demonstrating the achieved outcomes and effects.

setup (see figure 3(A)) involves placing all three light posts closer together with their LEDs activated. By guiding the light through the prism, which is achieved by placing the prism post/mount in front of the light sources, a distinct rainbow-like spectrum becomes apparent (refer to figure 3(B)). This experimental configuration can serve as an extension to elucidate the principles of light dispersion. To optimize screen visibility during the experiments, ambient lighting was intentionally dimmed.

3.2. Exploring energy conversion and reflection

The objective of this experiment is to comprehensively explore and effectively demonstrate the fundamental principles of reflection and the intriguing process of energy conversion involving solar cell detectors. It aims in showcasing the underlying principles behind the conversion of light energy into electrical energy, utilizing solar cells as the medium for this transformation. Additionally, this hands-on experiment also provides a tangible demonstration of how light can be harnessed to generate electricity through a phenomenon known as the photovoltaic effect. The experimental setup is illustrated in figure 4(A), featuring a configuration that includes a flashlight (serving as the light source), a 75 mm × 75 mm reflective surface (acting as a mirror), and solar cell detectors. The setup for the solar cell detectors involves the integration of two solar cells that are interconnected in parallel, subsequently linked to an LED indicator. Each of the above-mentioned components is securely mounted on designated 3D printed mounts (see figures 1(e)–(g)) designed to firmly hold them in place. The experimental arrangement involves placing the mounted reflective mirror onto the 3D printed optical breadboard and orienting the solar cell detectors at specific angles. The flashlight, functioning as the light

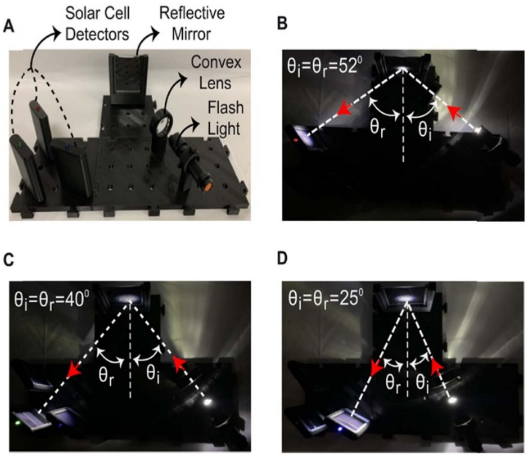

Figure 4. (A) Experimental arrangement for illustrating reflection and conversion of energy from light to electricity. Results demonstrating the effects at incident angles of (B) $\theta_i = 52°$, (C) $\theta_i = 40°$, and (D) $\theta_i = 25°$ on the reflective mirror.

source, is positioned at an angle to emit light onto the reflective mirror—known as the 'incident angle.' As a result, the light reflecting off the mirror is captured and detected by a solar cell detector, placed at an angle relative to the mirror's normal line. In this context, the term 'normal' signifies the perpendicular line drawn to the mirror's surface. To delve into the captivating interplay between the angle of reflection and the angle of incidence, we used three solar cells detectors positioned at varying angles. With careful manipulation of the flashlight holder's position, the reflected light is directed towards each of the solar cell detectors. As the light reaches the solar cell detectors, it imparts energy that activates the connected LEDs. This dynamic display effectively illustrates the fascinating phenomenon of energy conversion, where the energy carried by light in the form of photons undergoes seamless transformation into electrical energy, vividly bringing this fundamental principle to life before our eyes. Furthermore, we measured the angles of incidence and reflection in the experiment using a basic protractor. Here, we examined three incident angles: 52°, 40°, and 25° as shown in figures 4(B)–(D).

This experiment extends beyond its fundamental implications to serve as a portal to broader discussions. It stands as a versatile tool that initiates dialogues surrounding renewable energy, unveils the particle-like behaviour of light, and facilitates an in-depth exploration of solar cell functionality. Moreover, it opens the door to investigating the outcomes of connecting solar cells in both series and parallel arrangements, thereby endowing students with a comprehensive grasp of energy conversion mechanisms and their tangible applicability in real-world scenarios.

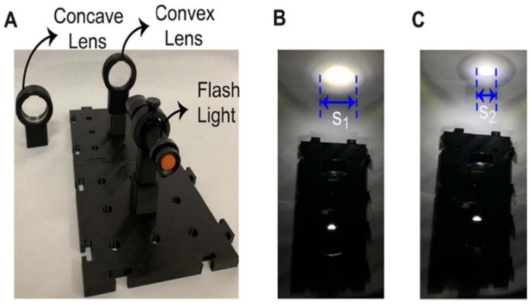

Figure 5. (A) Experimental setup to observe and demonstrate light divergence and convergence phenomena. (B) Result illustrating the divergence effect of light (i.e. light spreading). (C) Result displaying the convergence effect of light (i.e. light focusing). Figures B and C are placed side by side for easy comparison of the effects of convex and concave lenses.

3.3. *Demonstrating divergence and convergence of light*

Exploring the divergence and convergence properties of light holds immense significance across diverse scientific and technological domains. This endeavour grants us profound insights into the intricate behaviour of light rays as they interact with various optical components, encompassing lenses, mirrors, and prisms. This exploration fundamentally underpins the principles governing optics, unravelling the secrets that govern the behaviour of light in its journey through optical elements. To observe this unique behaviour exhibited by light rays as they traverse convex and concave lenses, unravelling the phenomena of convergence and divergence. To facilitate this investigation, an experimental setup is designed and modelled, as shown in figure 5(A). The setup comprises of the following components: convex and concave lenses, a light source (flashlight), and a white screen. Each of these components is securely positioned on 3D printed mounts tailored to their distinct geometries, ensuring stability and precise alignment (refer to figures 1(c) and (f)). The lenses utilized in this experiment are acrylic and possess a diameter of 38 mm. To observe the phenomenon of light convergence, the convex lens, securely placed within its mount, is positioned between the light source and the screen. Once the light source is activated, the light rays passing through the lens come together and converge, creating a distinctly sharp and focused spot of light on the screen. This observation captures the essence of convergence. Moving on to explore the phenomenon of light divergence, the convex lens is substituted with its concave counterpart. By directing the light emitted from the flashlight towards the concave lens, the light rays alter their trajectory upon passing through the concave lens. This leads to the formation of a dispersed pattern of light on the screen, which stands in stark contrast to the focused spot observed earlier. The figures 5(B) and (C) serve as visual depictions and direct observations of the convergence and divergence phenomena. In these illustrations, a crucial factor comes into play: the distance between the light source and the lens, as well as the distance between the lens and the screen. The distance remained consistent with both the convex and the concave scenarios. This intentional uniformity in distances facilitates a parallel comparison of the two distinct spots, enabling a clear assessment of the disparities between these two phenomena. Additionally using this setup, the focal length of a lens is determined using the common 'Lens Formula,' which is expressed as $\frac{1}{f} = \frac{1}{v} - \frac{1}{u}$. Here, '$v$' represents the distance between the lens and the screen, 'u' is the distance between the lens and the flashlight (or light source), and 'f' signifies the focal length of the lens. By manipulating these distances and applying the formula, the focal length of the lens can be accurately measured.

3.4. Exploring light diffraction and its phenomena

The phenomenon of diffraction presents one of the captivating behaviours of light, where it bends as it passes around an edge or through a narrow slit. This intriguing effect can be easily demonstrated using the 3D printed components designed for this purpose. To conduct this demonstration, we utilize the mounts showcased in figures 1(f) and (h), which are tailored to accommodate the green laser source ($\lambda = 532$ nm) and diffraction slit, respectively. The experimental arrangement involves, securely positioning the laser light source and the diffraction slit in their respective 3D printed mounts on the optical breadboard. The laser light source is aligned in front of the diffraction slit. The laser light passing through the slit is projected onto a distant wall, positioned at a substantial distance from the opposite end of the diffraction slit (as depicted in figure 6(A)). To observe the intriguing phenomenon of diffraction, we initially activated the laser without the presence of the diffraction slit. In this configuration, the laser light is projected directly onto the distant wall. However, when the diffraction slit is introduced, a fascinating change occurs in the behaviour of light. As shown in figure 6(B), the laser light passing through the diffraction slit diverges and bends around the edges of the opening. This intricate behaviour results in the formation of a pattern on the screen, with alternating bright and dark spots. Moreover, this experimental setup can be expanded to delve into the wave nature of light and explore the phenomenon of light interference, offering a comprehensive exploration of light's remarkable properties. Also, using this experiment, the distance between two slits

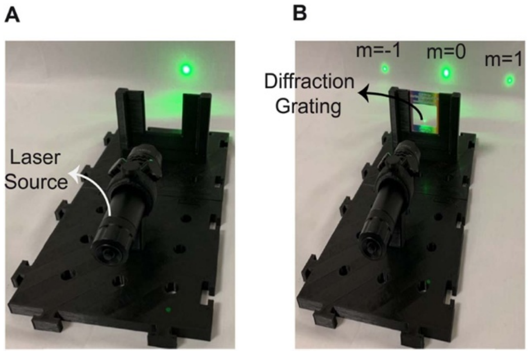

Figure 6. (A) Experimental setup to observe and demonstrate the concept of light diffraction phenomena, and the results showcasing the laser light effect without the diffraction grating. (B) Results illustrating the divergence effect when the diffracting grating is inserted into the mount's slot.

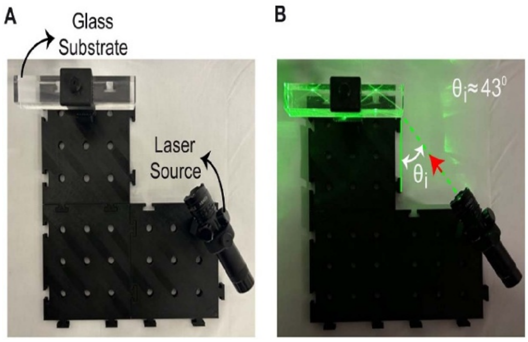

Figure 7. (A) Experimental setup to observe and demonstrate total internal reflection phenomena. (B) Results showcasing the effect of total internal reflection as the laser light travels within the rectangular prism.

can be measured using the formula $d = \lambda/\sin(\theta)$, where λ is the wavelength of the light beam, and θ is the angle between the central maxima and a bright spot. The angle θ can be determined using the relation $\theta = \arctan(y/D)$, where y is the distance between the central maxima and a bright spot, and 'D' is the distance from the grating to the screen. Our calculations yielded a slit distance (d) of 0.995 μm, which is very close to the manufacturer specified value, i.e. 1000 lines mm^{-1} which leads to 1 μm slit distance.

3.5. *Total internal reflection observation*

Total internal reflection is a captivating optical phenomenon that occurs when a light ray traveling within a medium encounters the boundary of another medium at an angle surpassing the critical angle. This results in the complete reflection of the light back into the original medium. This phenomenon finds extensive application in optical devices like prisms and optical fibres. To showcase the principle of total internal reflection, we employ a combination of components: a polymethyl methacrylate (PMMA) rod and a green laser source (λ = 532 nm). The experimental procedure involves precisely positioning the PMMA rod and the laser source using dedicated 3D printed holders, as shown in figures 1(f) and (i). These holders are placed on the 3D printed breadboard using the pegs, creating a stable setup. Laser source is positioned along with its holder at an inclined angle relative to the glass prism. This arrangement ensures that the light emitted by the laser strikes the surface of the PMMA rod at an angle falling within the critical range for total internal reflection. Above arrangement results in an experimental setup shown in figure 7(A). Additionally, the laser holder can facilitate rotation, enabling precise adjustments to the angle of incidence. Upon activating the laser source, the light traverses through the PMMA rod and encounters the boundary between the rod and the surrounding air. If the angle of incidence surpasses the critical angle for the glass-air interface, the phenomenon of total internal reflection manifests. The light rays are entirely reflected into the glass, generating an internal reflection phenomenon that is visually apparent (see figure 7(B)). We employed a protractor to determine the angle of incidence, which is referred to as the critical angle (θ_C). To compute the refractive index (n) of the denser medium, you can apply the essential formula: $n = {}^{1}/_{\sin(\theta_C)}$. This formula plays a pivotal role in comprehending how light behaves when transitioning between different media at an interface. From our measurements, we noticed $\theta_C \approx 43^0$ and $n \approx 1.47$. The expected value for PMMA rod refractive index is 1.5.

This experiment's intrigue grows as we manipulate the PMMA rods angle and the laser source's orientation, enabling to explore various scenarios and angles of incidence. Through this setup, students can effectively understand the core principles of optics and the practical applications of total internal reflection in diverse optical devices. The potential for expanding this setup to examine into related concepts such as the critical angle, Snell's law, and the principles of reflection and refraction is noteworthy.

3.6. *Observing LED and laser diode I–V characteristics*

Utilizing the designed 3D printed components described earlier, an experimental arrangement can be configured to effectively measure and observe the *I–V* characteristics of LEDs. LEDs are integral components of modern technology, playing a pivotal role in various applications such as lighting, displays, and communication devices. Understanding the *I–V* characteristics of LEDs is of paramount importance as they provide

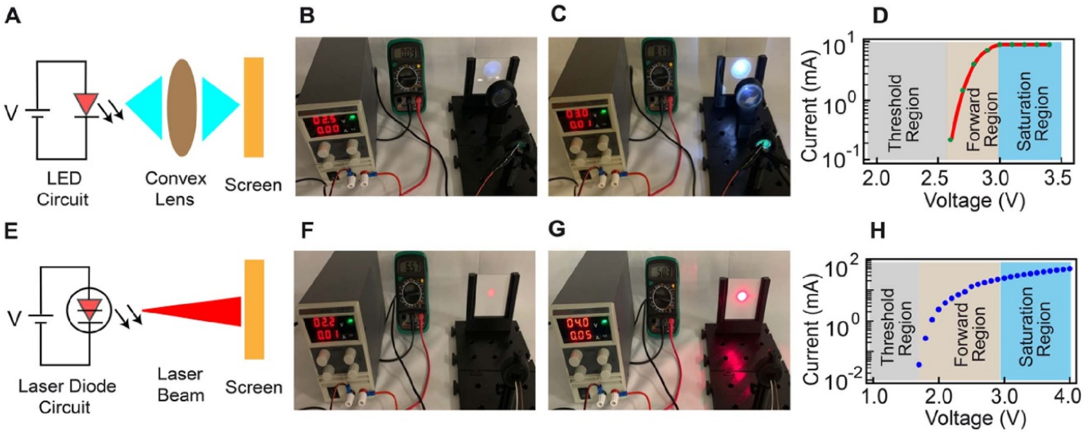

Figure 8. Experimental setup to characterize LED and laser diode IV characteristics. (A) Shows the setup schematic. (B) Depicts the application of threshold voltage to just illuminate the LED. (C) Demonstrates full LED illumination in the forward region of operation. (D) Displays the *I–V* plot of the LED, Highlighting different operational regions. (E) Shows the setup schematic. (F) Illustrates the setup for measuring the *IV* traits of the laser diode, emphasizing the threshold current. (G) Shows enhanced lasing with increased current in the forward region of operation. (H) Exhibits the *IV* plot of the laser diode, Featuring its varied operational regions. In (A) and (E), $V = 3$ V.

valuable insights into their behaviour under different voltage and current conditions. This information aids in optimizing LED performance, enhancing energy efficiency, and ensuring safe and reliable operation. By accurately assessing the *I–V* characteristics of LEDs, we gain a comprehensive understanding of their operational range, efficiency, and potential applications.

To investigate the *I–V* characteristics of an LED, we employ following components: an LED, a 100 ohm resistor, a DC power supply, and a multimetre. Soldered onto a circularly cut PCB board, the LED and resistor form a series connection. The resistor ensuring current limitation and damage prevention. The PCB board is secured within a circular holder (see figure 1(K)) and subsequently mounted onto a specialized 3D printed mount (see figure 1(K)). The setup (see figure 8(A)) is mounted on the 3D printed bread board and a convex lens, and a screen is placed in front of the LED mount. It is important to make sure which way are the LED's positive and negative ends are (anode and cathode). Also, it is recommended to note down the LED's details like how much voltage it needs and the maximum current it can handle. This helps to make sure the experiment does not go beyond what the LED can handle. In our case, the LED can handle up to 20 mA of current. For the experiment, the ammeter is connected in series with the LED and resistor. This helps to measure the current that flows through the LED. The voltmeter is connected across the LED to measure the voltage. At the same time, the power supply is connected to the circuit. The setup schematic is shown in figure 8(A). During the experiment, the power supply's voltage is gradually increased in small steps, ranging from 0.1 V up to 3.5 V. Correspondingly, current and voltage values are carefully recorded using the ammeter and voltmeter. This process continues until reaching the maximum current value, such as 20 mA. The resulting increase in LED brightness is easily visible on the screen. Afterward, the collected voltage and current data are plotted on an *I–V* characteristics graph, with voltage displayed on the horizontal *x*-axis and current on the vertical *y*-axis (see figure 8(D)). The plotted *I–V* curve reveals important information about how LEDs work. First, there's the 'Threshold Region' on the left side of the curve. Here, the LED does not let much current through until it reaches a specific voltage called the threshold voltage (Vth). That's when the LED forward biases. Next, we have the 'Forward Region.' It is a straight line on the curve where the LED works normally. When you increase the voltage, the current through the LED also goes up.

The slope of this line can tell us how efficient the LED is. Lastly, there's the 'Saturation Region.' In this area, the curve is not as steep, which means the LED is getting close to the saturation current it can handle. If you use the LED in this region, it can get very hot and may even break. The exact shape of the LED *I–V* curve can change depending on the type of LED. This simple experiment helps in providing valuable insights into the behaviour of LEDs, enhancing the understanding of its practical applications. For advanced optoelectronics courses, this information aids in optimizing LED performance, enhancing energy efficiency, and ensuring safe and reliable operation. By accurately assessing the *I–V* characteristics of LEDs, students can also gain a comprehensive understanding of their operational range, efficiency, and potential applications.

To investigate the *I–V* characteristics of a laser diode, we establish a controlled experimental setup. This setup entails the incorporation of key components, such as a red laser diode ($\lambda = 635$ nm), a DC power supply, and an ammeter/voltmeter. The red laser diode is carefully secured on a holder and mounted on the 3D printed mount (see figure 1(K)). It is essential to note the orientation of the diode's anode and cathode for proper connections. Specifications like the diode's forward voltage and maximum current rating are recorded to ensure the experiment operates within safe parameters. Connecting the ammeter in series with the laser diode-resistor circuit enables current measurement. The power supply is then linked to the circuit to provide variable DC voltage, while a voltmeter measures the voltage across the laser diode. The setup schematic is available for reference (see figure 8(E)). To witness the laser diode in operation, a screen is placed in front of it. We gain insights into the diode's behaviour by incrementally raising the voltage supplied by the power source in small increments, usually around 0.1 V, while simultaneously recording the associated current and voltage measurements until reaching 4 V. Using the collected data, we created a graph called the *I–V* characteristics graph (see figure 8(H)). This graph helps to identify important aspects of laser diode performance. First, there's a part on the left side of the graph known as the threshold region. In this region, the current flowing through the diode is very low until it reaches a minimum threshold called the 'threshold current' (I_{th}). During this phase, the diode is hardly activated, as observed in figure 8(F). Below this threshold, the laser diode does not emit coherent light. So, the I_{th} is the crucial current level where the laser diode starts emitting coherent light, and it is an important parameter for understanding laser diodes. Next, there's a linear region where increasing the voltage leads to more current until it reaches the diode's maximum current rating, which is called as the 'Forward Voltage.' At this point, the laser diode operates efficiently in its forward-biased mode, and you can see a brighter laser spot on the screen. At this juncture, a more luminous laser spot becomes visible on the screen (see figure 8(G)). It is worth noting that the exact shape of the laser diode IV curve can vary based on factors like the diode's type, wavelength, and design. However, this simplified curve gives us a general idea of the key regions and parameters when studying how a laser diode behaves. This experiment not only offers insights into laser diode behaviour but also enhances our understanding of their practical applications in various fields.

3.7. Exploring photodetection: a comparative study of photodiode, phototransistor, and photoresistor performances

Leveraging the custom 3D printed components as previously detailed, we established a practical setup to facilitate the observation of photodetection phenomena. This experiment entails conducting a comparative analysis involving three distinct photodetection elements: photodiode, phototransistor, and photoresistor. These components are affixed onto a circular PCB and securely positioned on the corresponding circular 3D printed mount (see figure 1(K)). The primary objective is to examine their respective responses to different light intensities.

To initiate the experiment, the photodiode integrated with the circular mount is securely attached to the designated 3D printed holder and positioned on the 3D printed breadboard. Figure 9(A) depicts the experimental setup. A red laser diode source ($\lambda = 635$ nm) is positioned

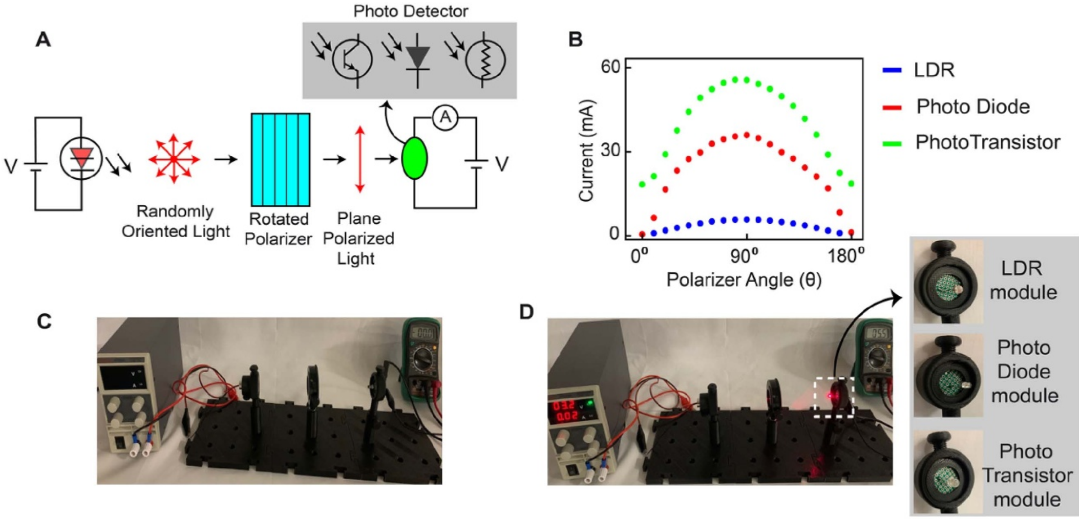

Figure 9. Experimental setup for characterizing LDR, photodiode, and phototransistor responses to light intensity. (A) Depicts the schematic representation of the setup, $V = 3$ V. (B) Demonstrates the response of LDR, photodiode, and phototransistor to varying light intensities, corresponding to the orientation of the polarizer. Illustrations of the experimental setup are shown in (C) when the laser is off and (D) when the laser is on. The insert showcases the LDR, photodiode, and phototransistor modules used in the experiment.

in front of the photodiode mount. To manipulate the light intensity of the incident light, a polarizer is positioned between the laser source and the photodiode module. The laser diode is powered with 3.2 V using a DC source. The photodiode is powered with a 3 V battery and additionally an ammeter is connected in series to the photodiode module (see the setup schematic in figure 9(A)). This configuration measures the current generated when the photons incident on the photodiode. The experimental setup is shown in figures C and D. Next, by systematically adjusting the orientation of the polarizer, the photodiode's response to varying light intensities, influenced by the angle (θ) of the polarizer, is measured. This involves recording the generated current by the photodiode. Once this phase is completed, the photodiode is replaced with a phototransistor module, and the experimental procedure is repeated. Like the previous step, the phototransistor's response to different light intensities, correlated to the polarizer's orientation, is recorded. Following this, the same procedure is repeated with the photoresistor module. Subsequently, the gathered data is plotted onto a single graph as shown in figure 9(B), facilitating a comparative analysis of the photodiode, phototransistor, and photoresistor performances.

The outcomes of this experiment contribute to a comprehensive understanding of photodetection principles and the unique attributes of each component. It also, allows to comprehend the current generation from these photodetection components to the incident light intensities. Furthermore, this study has the potential for extension to calculate critical parameters like quantum efficiencies, which are essential from an optoelectronics perspective. Overall, this study sheds light on the practical applications and advantages of different photodetection devices and serves as a valuable learning tool.

4. Advantages of 3D printed optical bench setup

The utilization of 3D printing technology for crafting the optical bench setup offers a triad of advantageous factors in comparison to procuring ready-made equipment from the market. Using 3D printed components can be a cost-effective choice compared to commercially available alternatives. This approach often leads to significant savings, ranging from hundreds to thousands of dollars, depending on the specific equipment needed. Table 1 provides a cost comparison between

Table 1. Overall cost of designing the 3D optical bench setup to conduct the proposed experiments.

Components sourced externally	Shown in	Cost in USD	3D printed Components	Shown in	Overall Weight in grams	Cost in USD
Acrylic Lens Kit	Figures 2(A) and 5(A)	17.00	4× Breadboards	Figure 1(A)	248	4.96
Solar Cells	Figure 3(A)	16.00	15× Breadboard Pegs	Figure 1(B)	12	0.24
9V Batteries	Figure 2(C)	13.00	2X Height-Adjustable Mounts	Figure 1(K)	14	0.28
9V connectors	Figure 2(C)	07.00	3× RGB Light Components	Figure 1(D)	129	2.58
Mirror	Figure 3(A)	08.00	Acrylic Prism Mount	Figure 1(J)	64	1.28
Diffraction Grating	Figure 6(B)	13.00	3× Solar Cell-LED Mounts	Figure 1(E)	60	1.2
PMMA Rod	Figure 7(A)	15.00	PMMA Rod Mount	Figure 1(I)	18	0.36
Acrylic Prism	Figure 3(A)	13.00	Mirror/Screen Mount	Figure 1(G)	25	0.5
Flashlights	Figure 5(A)	23.00	Concave Lens Mount	Figure 1(C)	14	0.28
Green Laser	Figure 7(B)	50.00	Convex Lens Mount	Figure 1(C)	12	0.24
Red Laser	Figure 8(G)	06.00	2× Light/Laser Mounts	Figure 1(F)	18	0.36
Multimetre	Figure 8(G)	30.00	2× Height Extenders	Figure 1(K)	13	0.26
DC Power Supply	Figure 8(G)	50.00	3× PCB Ring Mounts	Figure 1(K)	2	0.04
Polarizer	Figure 9(C)	52.00	DC Laser source Mount	Figure 1(K)	15	0.3
Laser Diode	Figure 8(F)	12.00	Rectangular PCB Mount	Figure 1(K)	3	0.06
CR2032 connectors	Figure 9(C)	06.00	Diffraction Slit Mount	Figure 1(H)	23	0.46
CR2032 batteries	Figure 9(C)	06.00				
LEDs	Figures 2(C), 4(A), and 9(B)	06.00	**Total weight of 3D printed components: ∼670 grams. Total cost of 3D printed components: $13.40**			
100 Ω resistors	Figure 2(C)	05.00				
Total cost of purchased components: $348						

3D printed components and commercially purchased ones used in these experiments, highlighting the generally reasonable expenses associated with producing the 3D printed components. While aftermarket products may seem pricey initially, considering options like bulk purchases or choosing vendors with competitive pricing can help reduce overall costs. Additionally, the table includes the weights of the 3D printed components to illustrate the overall lightweight nature of the 3D optical experimental setup. The second major advantage pertains to the robustness of 3D printed optics mounts and equipment. Unlike factory-made counterparts, these printed components exhibit a remarkable resilience, owing partly to their economical production. In the event of a breakage, a 3D printed piece can be promptly reprinted without the need to wait for shipping, thus circumventing downtimes. Moreover, the replacement cost remains a fraction of what one would incur when ordering anew from equipment manufacturers. The third pivotal advantage lies in the expandability offered by 3D printing. Students and educators, irrespective of their proficiency in CAD software, can readily design novel components to extend the experiment repertoire. This expandability empowers the creation of fresh experiments to elucidate procedures and concepts, fostering heightened engagement in the subject matter. In essence, the trifecta of affordability, durability, and expandability positions 3D printing as a transformative tool, rendering optics education more accessible, innovative, and cost-efficient.

5. Conclusion

The utilization of the proposed 3D printed optical components has yielded a high degree of adjustability, culminating in the creation of an almost entirely 3D printed optical bench setup. By fabricating suitable 3D printed mounts and accompanying equipment, we effectively showcased numerous fundamental optical concepts encompassing light wavelength/colour, the electromagnetic spectrum, solar cells, reflection, convex/concave lenses, and diffraction. The outcomes of these demonstrations are meticulously detailed within this manuscript, underscoring the efficacy of the principles being illustrated. These experiments, designed with simplicity and safety in mind (with appropriate safety measures when utilizing lasers), are accessible to students of varying age groups, including those in grade schools. To facilitate further exploration and collaboration, the CAD files for the 3D printed optical components and systems have been made readily available online, providing a platform for collaboration, modification, and enhancement with additional innovative ideas.

Data availability statement

The data that support the findings of this study are openly available at the following URL/DOI: https://github.com/vinnakota5279/Open-Source-3D-Printed-Laboratory-for-optics-Education.

Acknowledgments

Raj Vinnakota and Brady Barr gratefully acknowledge funding from the National Science Foundation ERI (Award No. ECCS-2138198).

Author contributions

R V played a key role in developing and executing the idea, which involved analyzing the 3D models, 3D prints, and contributing to the manuscript's writing. B B was primarily responsible for designing the 3D models and 3D printing the components. Additionally, S R made contributions to the writing of the manuscript and setting up experiments.

Conflict of interest

The authors declare that they have no competing interests.

ORCID iD

Raj K Vinnakota https://orcid.org/0000-0003-4616-576X

Received 19 October 2023, in final form 4 December 2023
Accepted for publication 20 December 2023
https://doi.org/10.1088/1361-6552/ad1769

References

[1] Born M and Wolf E 2013 *Principles of Optics: Electromagnetic Theory of Propagation, Interference and Diffraction of Light* 3rd edn (Pergamon)

[2] Saleh B E A and Teich M C 2007 *Fundamentals of Photonics* 2nd edn (Wiley)
[3] Yariv A 2006 *Optoelectronics in Modern Communications* 6th edn (Oxford University Press)
[4] Kasap S O and Ruda H 2012 *Optoelectronics and Photonics: Principles and Practices* 2nd edn (Pearson)
[5] Opto-electronics market—growth, trends, and forecasts (2022–2032) (available at: www.precedenceresearch.com/optoelectronics-market#:∼:text=The%20global%20optoelectronics%20market%20size,period%20from%202023%20to%202032)
[6] Patricia D The optics workforce: looking to the future (available at: www.optica-opn.org/home/articles/volume_28/july_august_2017/features/the_optics_workforce_looking_to_the_future/)
[7] Galili I 2014 Teaching optics: a historico-philosophical perspective *International Handbook of Research in History, Philosophy and Science Teaching* ed M Matthews (Springer) pp 97–128
[8] Galili I and Hazan A 2000 Learners' knowledge in optics: interpretation, structure and analysis *Int. J. Sci. Educ.* **22** 57–88
[9] Clark R, Wang M, Zaghloul M, Sullivan S and Chen K 2019 'Project-based learning of optics and photonics: how to teach a stand-alone technical elective 'Niche' Course?' *2019 ASEE Annual Conf. & Exposition* (https://doi.org/10.18260/1-2–33207)
[10] Pompea S M and Stepp L 1995 Great idea for teaching optics *Proc. SPIE* **2525** 168–72
[11] Guzik R P 2004 A tutorial on light and optics for grade school teachers *Opt. Photon. News* **15** 18–21 (available at: www.optica-opn.org/home/articles/volume_15/issue_6/departments/education/education/)
[12] Varshneya R and DeGroote J 2004 An encounter with optics for grade school students *Opt. Photon. News* **15** 16–17 (available at: www.optica-opn.org/home/articles/volume_15/issue_11/departments/education/education/)
[13] Costa M F M, Sporea D and Clementina T 2005 Optics education in the frame of the Comenius 'hand-on science' project *Proc. SPIE* **9664** 96642A
[14] Magnani N and Donnelly J 2007 Innovative methods to teach optics in the grade 5 classroom *Proc. ETOP 2007* (*Ottawa, Canada*) pp 151–9
[15] Takayama O, Niederberger A, Ghenuche P, Mathew M and Volpe G 2007 El d'ia de la luz (the day of light) -two hours optics demonstration for secondary school students *Proc. ETOP 2007* (*Ottawa, Canada*) pp 160–5
[16] Lones J J, Maltseva N K and Peterson K N 2007 Science and fun in a "magic show of light" from optical demonstrations on an overhead projector for elementary school student *Proc. ETOP 2007* (*Ottawa, Canada*) pp 429–34
[17] Kruglak H 1991 The compact disc as a diffraction grating *Phys. Educ.* **26** 255–6
[18] Márquez A, Álvarez M L N, Méndez D and Beléndez A 2005 Effective physical optics hands-on experience through the characterization of a CD and a DVD *Proc. ETOP 2005* (*Marseille, France*, *24–27 October 2005*) pp 181–3
[19] Mejías P M, Martínez-Herrero R, Serna J and Piqueo G, 2005 Low-cost home experiments and demonstrations in optics *Proc. ETOP 2005* (*Marseille, France*, *24–27 October 2005*) pp 60–61
[20] Pompea S M, Johnson A, Arthurs E and Walker C E 2005 Hand-on optics: an educational initiative for exploring light and color in after-school programs, museums, and hand-on science centers *Proc. ETOP 2005* (*Marseille, France*, *24–27 October 2005*) pp 276–8
[21] Pompea S M and Walker C E 2005 Design and evaluation of optics student competitions and contests for maximal educational value *Proc. ETOP 2005* (*Marseille, France*, *24–27 October 2005*) pp 288–91
[22] Dyomin V V and Polovtsev G 2007 Educational kit for optical experiments *Proc. ETOP 2007* (*Ottawa, Canada*, *3–5 June 2007*) pp 310–20
[23] Ashok P C, James J, krisha Y, Chacko J V and Nampoori V P N 2009 Development of optics kit for schools in developing countries – International school of photonics model *Education and Training in Optics and Photonics* (*OSA Technical Digest Series (CD)*) (Optica Publishing Group) paper ESB5 (https://doi.org/10.1364/ETOP.2009.ESB5)
[24] Brecher K 2007 Project LITE: light Inquiry through experiments *Proc. ETOP 2007* (*Ottawa, Canada*, *3–5 June 2007*) pp 166–74
[25] Jacobs S D, Gregg L L, Andrews C M and Coppens R L, Optics suitcase: educational outreach presentation guide (available at: www.opticsexcellence.org) (Accessed December 2008)
[26] Animations for Physics and Astronomy Catalog for: optics Animations by Penn State University (available at: https://phys23p.sl.psu.edu/phys_anim/Phys_anim.htm)
[27] Physics and Chemistry by a clear learning (available at: www.physics-chemistry-interactive-flash-animation.com/optics_interactive.htm)
[28] Light and Optics Animations (available at: www.schoolphysics.co.uk/animations/Light%20and%20optics%20animations/)

[29] Virtual teaching resources for geometric optics (available at: https://phet.colorado.edu/en/simulations/geometric-optics)

[30] Brian D R 2017 A systematic review of the empirical research on selected aspects of homeschooling as a school choice *J. Sch. Choice* **11** 604–21

[31] Research facts on homeschooling, homeschool fast facts (available at: www.nheri.org/research-facts-on-homeschooling/)

[32] 3D printing of rocket engine components (available at: www.nasa.gov/centers/marshall/news/releases/2020/future-rocket-engines-may-include-large-scale-3d-printing.html)

[33] Brake caliper produced using 3D printer (available at: www.bugatti.com/media/news/2018/world-premiere-brake-caliper-from-3-d-printer/)

[34] Europe's first 3D printed house (available at: www.bouygues-construction.com/en/achievements/yhnova-house-printed-3d)

[35] Murphy S and Atala A 2014 3D bioprinting of tissues and organs *Nat. Biotechnol.* **32** 773–85

[36] Griffith K M, de Cataldo R and Fogarty K H 2016 Do-It-Yourself: 3D Models of Hydrogenic Orbitals through 3D Printing *J. Chem. Educ.* **93** 1586–90

[37] Smiar K and Mendez J D 2016 Creating and using interactive, 3DPrinted models to improve student comprehension of the Bohr model of the atom, bond polarity, and hybridization *J. Chem. Educ.* **93** 1591–4

[38] Robertson M J and Jorgensen W L 2015 Illustrating concepts in physical organic chemistry with 3D Printed Orbitals *J. Chem. Educ.* **92** 2113–6

[39] Rossi S, Benaglia M, Brenna D, Porta R and Orlandi M 2015 Three dimensional (3D) printing: a straightforward, user-friendly protocol to convert virtual chemical models to real-life objects *J. Chem. Educ.* **92** 1398–401

[40] Rodenbough P P, Vanti W B and Chan S-W 2015 3D-printing crystallographic unit cells for learning materials science and engineering *J. Chem. Educ.* **92** 1960–2

[41] Kaliakin D S, Zaari R R and Varganov S A 2015 3D printed potential and free energy surfaces for teaching fundamental concepts in physical chemistry *J. Chem. Educ.* **92** 2106–12

[42] Meyer S C 2015 3D printing of protein models in an undergraduate laboratory: leucine zippers *J. Chem. Educ.* **92** 2120–5

[43] Sathish T, Vijayakumar M D and Krishnan Ayyangar A 2018 Design and fabrication of industrial components using 3D printing *Mater. Today: Proc.* **5** 14489–98

[44] Boboc R and Antonya C 2021 Using 3D printing and augmented reality for teaching and learning in mechanical engineering higher education *EDULEARN21 Proc.* (https://doi.org/10.21125/edulearn.2021.0236)

[45] Shu J, Luo H, Zhang Y and Liu Z 2021 3D printing experimental validation of the finite element analysis of the maxillofacial model *Front. Bioeng. Biotechnol.* **9** 694140

[46] Gul J Z, Sajid M, Rehman M M, Siddiqui G U, Shah I, Kim K-H, Lee J-W and Choi K H 2018 3D printing for soft robotics – a review *Sci. Technol. Adv. Mater.* **19** 243–62

[47] Espalin D, Muse D W, MacDonald E and Wicker R B 2014 3D Printing multifunctionality: structures with electronics *Int. J. Adv. Manuf. Technol.* **72** 963–78

[48] Baden T, Chagas A M, Gage G, Marzullo T, Prieto-Godino L L and Euler T 2015 Open labware: 3D printing your own lab equipment *PLoS Biol.* **13** e1002086

[49] Pandey S, Gupta B and Nahata A 2013 Terahertz plasmonic waveguides created via 3D printing *Opt. Express* **21** 24422–30

[50] Busch S F, Weidenbach M, Fey M, Schäfer F, Probst T and Koch M 2014 Optical properties of 3D printable plastics in the THz regime and their application for 3D printed THz optics *J. Infrared Millim. Terahertz Waves* **35** 993–7

[51] Stewart C and Giannini J 2016 Inexpensive, open source epifluorescence microscopes *J. Chem. Educ.* **93** 1310–5

[52] Zhang C, Anzalone N C, Faria R P and Pearce J M 2013 Open-source 3D-printable optics equipment *PLoS One* **8** e59840

[53] Davis E J, Jones M, Alex Thiel D and Pauls S 2018 Using open-source, 3D printable optical hardware to enhance student learning in the instrumental analysis laboratory *J. Chem. Educ.* **95** 672–7

[54] To access Autodesk Fusion 360 (available at: https://help.autodesk.com/view/fusion360/ENU/?guid=GUID-297688D0-3512-4313-B4E5-0C4BD5AEFC7A)

[55] To access Autodesk Fusion 360 student version (available at: www.autodesk.com/support/account/education/students-educators/overview)

[56] Source page to the design files used to develop the bench setup (available at: https://github.com/vinnakota5279/Open-Source-3D-Printed-Laboratory-for-optics-Education)

[57] For Creality V3 3D printer (available at: www.creality3dofficial.com/collections/3d-printer)

[58] To access slicing software Ultimate Cura (available at: https://ultimaker.com/software/ultimaker-cura)

Dr Raj Vinnakota is an Assistant Professor and coordinates the Electronics Engineering Technology program at Troy University in Alabama, USA. He earned his Ph.D. in Engineering (concentration in Engineering Physics) from Louisiana Tech University. Dr Vinnakota's research focuses on Novel Optoelectronic Devices, Metal and Semiconductor-based Plasmonics, enhanced light-matter interactions, Nanophotonics, and Heat Transfer. Beyond his scientific pursuits, he is passionate about proposing innovative tools to elevate STEM education, especially in the Applied Physics, focusing on the fields of optics and optoelectronics. With a strong background in these disciplines, Dr Vinnakota is enthusiastic to introducing creative methodologies that enhance the learning experience for students.

Brady Barr, an undergraduate student at Troy University, focuses on additive manufacturing, optics, and electronics in his research. Recognized with the Chancellor's Award, he excels academically and explores practical applications of additive manufacturing, especially in optics and electronics. Proficient in parametric 3D modelling, Brady aims to expand his skills and merge optics, semiconductor physics, and additive manufacturing for innovative applications.

Sai Radavaram received his B.E. degree in Electrical and Electronics Engineering from Anna University, Chennai, India, in 2013, and his M.Sc. and Ph.D. degrees in Electrical and Computer Engineering from The University of Alabama in Huntsville, Huntsville, AL, USA, in 2015 and 2021, respectively. From 2016 to 2017, he was a Programmer Analyst at Genpact, Richardson, TX. From 2021 to 2023, he served as an Instructor in the Electronics Engineering Department at Troy University, Troy, AL. His research interests include Applied electromagnetics, RF and Microwave engineering, Wideband reconfigurable antennas, and Phased array antennas.